

## Structure of the snake-venom toxin convulxin

Thil Batuwangala,<sup>a</sup> Mireille Leduc,<sup>b†</sup> Jonathan M. Gibbins,<sup>c</sup> Cassian Bon<sup>b</sup> and E. Yvonne Jones<sup>a\*</sup>

<sup>a</sup>Cancer Research UK Receptor Structure Group, Division of Structural Biology, University of Oxford, The Henry Wellcome Building for Genomic Medicine, Roosevelt Drive, Headington, Oxford OX3 7BN, England, <sup>b</sup>Unité des Venins, Institut Pasteur, 25 Rue du Docteur Roux, 75724 Paris CEDEX 15, France, and <sup>c</sup>School of Animal and Microbial Sciences University of Reading, Whiteknights, PO Box 228, Reading, Berkshire RG6 6AJ, England

† Present address: Unité de Génétique et de Biochimie du Développement, Institut Pasteur, 25 Rue du Docteur Roux, 75724 Paris CEDEX 15, France.

Correspondence e-mail: yvonne@strubi.ox.ac.uk

Snake venoms contain a number of proteins that interact with components of the haemostatic system that promote or inhibit events leading to blood-clot formation. The snake-venom protein convulxin (Cvx) binds glycoprotein (GP) VI, the platelet receptor for collagen, and triggers signal transduction. Here, the 2.7 Å resolution crystal structure of Cvx is presented. In common with other members of this snake-venom protein family, Cvx is an  $\alpha\beta$ -heterodimer and conforms to the C-type lectin-fold topology. Comparison with other family members allows a set of Cvx residues that form a concave surface to be putatively implicated in GPVI binding. Unlike other family members, with the exception of flavocetin-A (FL-A), Cvx forms an  $(\alpha\beta)_4$  tetramer. This oligomeric structure is consistent with Cvx clustering GPVI molecules on the surface of platelets and as a result promoting signal transduction activity. The Cvx structure and the location of the putative binding sites suggest a model for this multimeric signalling assembly.

## 1. Introduction

Convulxin (Cvx) is a multimeric protein from the venom of *Crotalus durissus terrificus* and a powerful activator of platelets (Vargaftig *et al.*, 1980, 1983). It is a member of a group of snake-venom proteins affecting blood coagulation and is an  $\alpha\beta$ -heterodimer belonging to the C-type lectin family (Drickamer, 1988; Leduc & Bon, 1998). Early structural studies by electron microscopy suggested that the Cvx  $\alpha\beta$ -heterodimer forms a disulfide-linked multimeric ring-like structure (Marlas *et al.*, 1983*a,b*; Marlas, 1985). The functional effects of Cvx on platelets arises from its ability to bind with high affinity to the platelet receptor for collagen, glycoprotein (GP) VI (Francischetti *et al.*, 1997). Partial reduction of Cvx to disrupt its multimeric structure and subsequent incubation with platelets prevents collagen binding to GPVI (Polgar *et al.*, 1997). It has been proposed that the multimeric structure of Cvx causes clustering of GPVI and that this plays a major role in its activation. Thus, the multimeric structure of Cvx could act in a similar manner to the structural repeats in collagen (Polgar *et al.*, 1997; Clemetson & Clemetson, 2001). At the platelet cell surface GPVI is present in complex with the F<sub>c</sub>-receptor  $\gamma$ -chain and this complex has been shown to be essential for signal transduction (Poole *et al.*, 1997; Berlanga *et al.*, 2002; Nieswandt & Watson, 2003). Signal transduction events induced by Cvx have been shown to be similar to those induced by collagen or collagen-like peptides (Achison *et al.*, 1996) and to involve time-dependent tyrosine phosphorylation of the F<sub>c</sub>-receptor  $\gamma$ -chain, phospholipase C $\gamma$ 2, p72<sup>SYK</sup>, c-Cbl, p36-38 (Polgar *et al.*, 1997), P13 kinase and PKB (Barry &

Received 22 August 2003  
Accepted 30 September 2003

**PDB Reference:** convulxin,  
1uos, r1uossf.

**Table 1**  
Crystallographic data statistics.

Values in parentheses are for the outermost resolution shell (2.80–2.70 Å for ID-14 EH2 and 3.11–3.00 Å for SRS 9.6 data sets).

| Data collection                               | ESRF ID-14 EH2   | SRS 9.6  |
|---|--|--|
| Space group                                   | <i>I4</i>  | <i>I4</i>  |
| Unit-cell parameters (Å, °)                   | $a = b = 133,$<br>$c = 113,$<br>$\alpha = \beta = \gamma = 90$ | $a = b = 130,$<br>$c = 111,$<br>$\alpha = \beta = \gamma = 90$ |
| Resolution range (Å)                          | 20–2.7   | 20–3.0   |
| Completeness (%)                              | 99.9 (99.9)  | 100.0 (100.0)  |
| Total observations                            | 154959   | 118553   |
| Unique reflections                            | 27008  | 18469  |
| Average $I/\sigma(I)$                         | 10.2 (2.7)   | 14.8 (2.9)   |
| $R_{\text{merge}}^{\dagger}$ (%)              | 20.5 (48.4)  | 15.0 (72.8)  |
| Model refinement                              |  |  |
| Maximum resolution (Å)                        | 2.7  |  |
| Reflections (working set/test set) $\ddagger$ | 25837/908  |  |
| $R_{\text{work}}/R_{\text{free}}^{\S}$ (%)    | 20.5/24.5  |  |
| R.m.s.d. from standard stereochemistry        |  |  |
| Bonds (Å)                                     | 0.010  |  |
| Angles (°)                                    | 1.5  |  |
| No. of protein atoms                          | 4288   |  |
| No. of water atoms                            | 320  |  |
| Mean $B$ factors (Å <sup>2</sup> )            |  |  |
| Protein                                       | 48.7   |  |
| Water   | 51.4   |  |
| Ramachandran plot, residues in                |  |  |
| Most favoured regions (%)                     | 85.3   |  |
| Additional allowed regions (%)                | 13.7   |  |
| Generously allowed regions (%)                | 0.4  |  |
| Disallowed regions (%)                        | 0.6  |  |

$\dagger R_{\text{merge}} = \sum_h \sum_i |I_i(h) - \langle I(h) \rangle| / \sum_h \sum_i I_i(h)$ , where  $I_i(h)$  is the  $i$ th measurement of reflection  $h$  and  $\langle I(h) \rangle$  is the weighted mean of all measurements of  $h$ .  $\ddagger$  All reflections with  $F > 0$  were included.  $\S R = \sum_h ||F_{\text{obs}}| - |F_{\text{calc}}|| / \sum_h F_{\text{obs}}$ , where  $F_{\text{obs}}$  and  $F_{\text{calc}}$  are the observed and calculated structure-factor amplitudes, respectively.  $R_{\text{free}}$  is as  $R_{\text{work}}$  but calculated for a test set comprising reflections not used in refinement.

Gibbins, 2002). However, additional signal transduction proteins in platelets, normally phosphorylated by collagen activation (such as pp125<sup>FAK</sup>), are not phosphorylated by Cvx binding (Polgar *et al.*, 1997). These differences may lie in the ability of collagen to bind a range of platelet receptors. Whilst Cvx predominantly interacts with platelets *via* GPVI, collagen has additional interactions with GPIa/IIa and CD36 (Polgar *et al.*, 1997). As a result of this, there are differences in the strength and timing of the signal transduction events triggered by Cvx and those triggered by collagen, although the overall pattern of tyrosine phosphorylation is similar (Polgar *et al.*, 1997). In a recent report, Cvx has been shown to also bind platelet GP1b $\alpha$  (Kanaji *et al.*, 2003). Since this receptor also has a central role in platelet response and thrombus formation, it is possible that the stimulatory effects of Cvx on platelets may at least in part be attributable to the binding of this second receptor.

Snake-venom toxins are commonly used as tools in the study of platelet-receptor interactions. Cvx was instrumental in the cloning of GPVI (Clemetson *et al.*, 1999) and has had a major impact on the understanding of GPVI-regulated signalling (Polgar *et al.*, 1997; Poole *et al.*, 1997; Cicmil *et al.*, 2000; Barry & Gibbins, 2002; Berlanga *et al.*, 2002). To gain further insights into the function of Cvx and its interaction with GPVI, we determined the molecular structure of Cvx by

X-ray crystallography, built a homology model of GPVI and identified residues that could be involved in the interaction.

## 2. Materials and methods

### 2.1. Crystallization, structure determination and analysis

The convulxin protein was purified as previously described (Francischetti *et al.*, 1997). Crystallization conditions were screened using purified Cvx at a concentration of 1 mg ml<sup>-1</sup> in 10 mM Tris–HCl pH 8.0, 10 mM NaCl. Nanolitre-scale crystallization experiments were set up using a Cartesian Technologies Microsys MIC4000 (Genomic Technologies, Huntingdon; England; Brown *et al.*, 2003; Walter *et al.*, 2003). Conditions yielding crystals in nanolitre-scale sitting drops (100 nl protein plus 100 nl reservoir solution) were subsequently scaled up and optimized by hand pipetting. Optimally diffracting crystals were grown at 277 K from 2  $\mu$ l sitting drops using a 1:1 protein to precipitant (100 mM sodium acetate pH 4.0, 20–30% 1,4-butanediol) ratio.

Crystals were flash-frozen at 100 K within seconds of transfer to mother liquor containing 20–25% glycerol. Data sets were collected on ADSC Q4 CCD detectors at beamlines 9.6 (SRS, Daresbury, England) and ID-14 EH2 (ESRF, Grenoble, France) using radiation with wavelengths of 0.86 and 0.93 Å, respectively. The data were processed using *DENZO*, *SCALEPACK* (Otwinowski & Minor, 1997) and *TRUNCATE* (Collaborative Computational Project, Number 4, 1994). Processing statistics are given in Table 1. The crystals belong to space group *I4* and diffracted to 3.0 Å at SRS 9.6 (with unit-cell parameters  $a = b = 130.0$ ,  $c = 111.1$  Å) and to 2.7 Å at ID-14 EH2 (with unit-cell parameters  $a = b = 132.5$ ,  $c = 113.0$  Å). The Cvx structure was solved from data collected at SRS 9.6 by molecular replacement using *CNS* (Brünger *et al.*, 1998) using the coordinates of factor IX-bp (an  $\alpha\beta$ -heterodimer; PDB code 1bj3; Mizuno *et al.*, 1999) as the search model.

The crystallographic asymmetric unit contains two molecules of Cvx with a solvent content of 71%. After rigid-body refinement of the molecular-replacement solution coordinates (treating the  $\alpha$ - and  $\beta$ -chains as two separate rigid bodies), the protein backbone was rebuilt in *O* (Jones *et al.*, 1991). Protein side chains of the molecular-replacement model were mutated to the amino-acid sequence of Cvx using the program *MUTATE* (R. Esnouf, unpublished work) and positioned within electron density using *O*. The Cvx model was built using data collected at SRS 9.6 with reference to  $2F_o - F_c$  electron-density maps that were twofold averaged and solvent-flattened in *GAP* (D. I. Stuart and J. M. Grimes, unpublished work).

This model was further refined in *CNS* (Brünger *et al.*, 1998) using higher resolution data collected at ID-14 EH2. For the initial cycles of positional refinement strict non-crystallographic symmetry constraints were retained, after which positional and individual  $B$ -factor refinement was carried out using non-crystallographic symmetry restraints. Water molecules were picked automatically using *CNS* and manually

verified. Protein stereochemistry was validated using *PROCHECK* (Laskowski *et al.*, 1993). The final statistics of the refined model are given in Table 1.

For the analysis of the protein structure, molecular surfaces were calculated using the program *VOLUMES* (R. Esnouf, unpublished program). For comparative analysis, coordinates of homologous structures were superimposed with *SHP* (Stuart *et al.*, 1979). Sequence alignments were performed using the *MULTALIN* web interface (Corpet, 1988) and the output formatted with *ESPRIT* (Gouet *et al.*, 1999).

The GPVI structure was modelled with *SWISS-MODEL* using the coordinates of Lir-1 (PDB code 1g0x; Chapman *et al.*, 2000), with which it shares 44% sequence identity. Structural analysis was carried out using the programs *O* and *VMD* (Humphrey *et al.*, 1996). Electrostatic potentials on the protein surface were calculated and visualized with the program *GRASP* (Nicholls *et al.*, 1991). Figures were produced using *BOBSCRIPT* (Esnouf, 1999), *Raster3D* (Merritt & Bacon, 1997) and *GRASP*.

### 3. Results and discussion

#### 3.1. Overall structure of Cvx

The backbone conformation of the two non-crystallographic symmetry-related  $\alpha\beta$ -heterodimers differs by a root-

mean-square deviation (r.m.s.d) value of 0.33 Å and is reduced to a value of 0.16 Å with residues 61 and 62 of the  $\beta$ -subunit excluded. All structural analyses were carried out on one of the two equivalent  $\alpha\beta$ -heterodimers (chains *A* and *B* in the PDB coordinates).

The  $\alpha$ - and  $\beta$ -subunits of Cvx have 38% sequence identity and are structurally homologous. Each Cvx subunit has a C-type lectin fold and the heterodimer is formed by domain swapping, as observed in the structures of other snake-venom proteins of this family (Mizuno *et al.*, 1997, 1999, 2001; Fukuda *et al.*, 2000; Hirotsu *et al.*, 2001; Sen *et al.*, 2001). Although the C-type lectin-like snake-venom proteins have sequence homology to classic C-type lectins, formation of the domain-swapped heterodimer results in the disruption of the lectin active site and consequent loss of lectin activity (Mizuno *et al.*, 1997; Drickamer, 1988). Several modes of oligomerization have been observed in C-type lectin proteins (Drickamer, 1988) and the domain-swapped head-to-head interaction was first observed in the structure of factor IX/X-bp (Mizuno *et al.*, 1997). The C-type lectin family of snake-venom proteins is one of the most structurally divergent members of the C-type lectin superfamily (Drickamer, 1988).

The  $\alpha$ - and  $\beta$ -subunits of Cvx are related by a pseudodyad which is perpendicular to the long axis of the  $\alpha\beta$ -heterodimer (Fig. 1*a*). This heterodimer is stabilized by an interchain

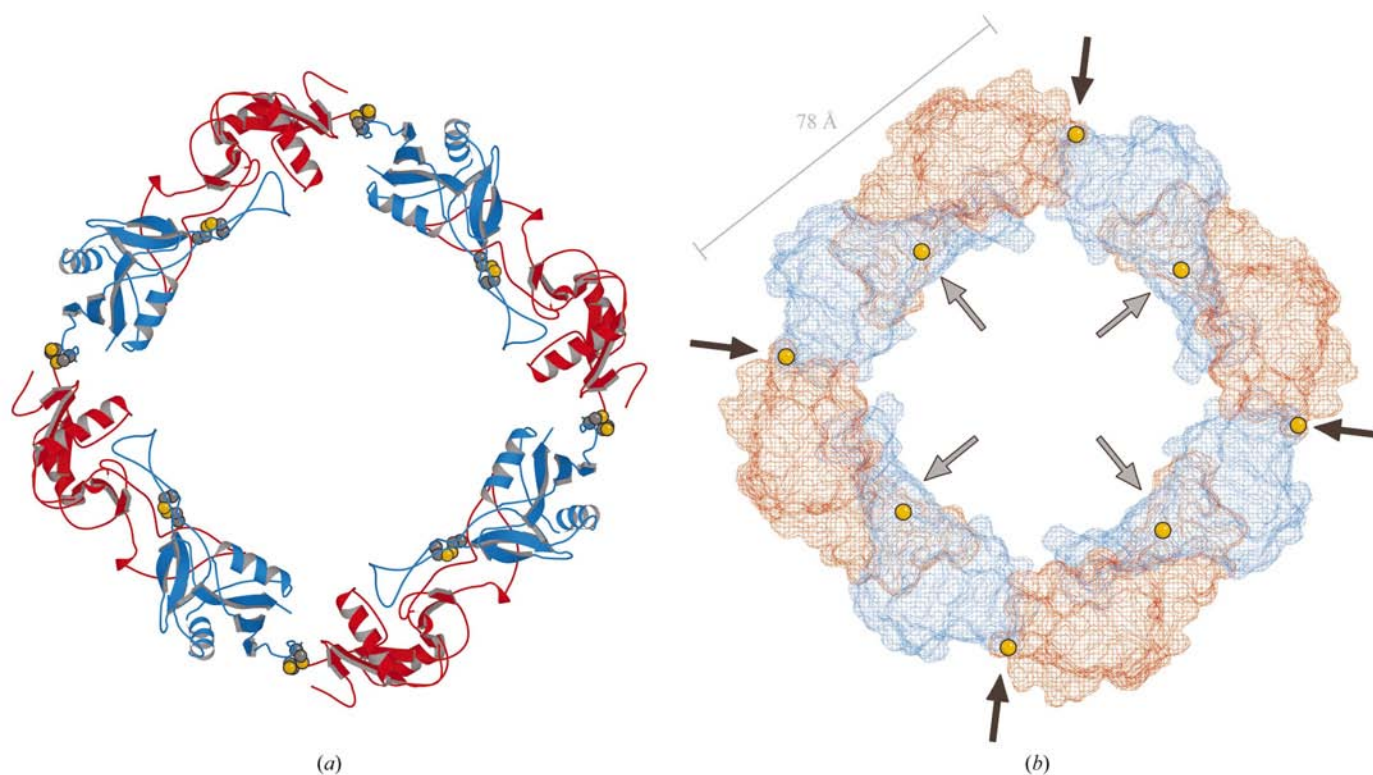


**Figure 1**

Oligomeric structure of convulxin. (*a*) The overall structure of the Cvx ( $\alpha\beta$ )<sub>4</sub> tetramer is depicted schematically in ribbon representation with the  $\alpha$ -subunit coloured red and the  $\beta$ -subunit blue. The side chains of the cysteine residues forming the intra-subunit disulfide bridges linking the domain-swapped  $\alpha\beta$ -heterodimer and those forming the inter-subunit disulfide bridges linking the ( $\alpha\beta$ )<sub>4</sub> tetramer are depicted as van der Waals spheres (carbon in grey; sulfur in yellow). (*b*) Surface representation of the Cvx ( $\alpha\beta$ )<sub>4</sub> tetramer. The molecular surface is drawn in mesh ( $\alpha$ -subunit, red;  $\beta$ -subunit, blue). The positions of disulfide bridges linking the tetramer are drawn as yellow spheres and indicated by arrows (intra-subunit in grey; inter-subunit in black). The distance between pairs of inter-subunit disulfide bonds is marked.

disulfide bond formed between Cys79 of the  $\alpha$ -subunit and Cys76 of the  $\beta$ -subunit (Fig. 1*a*). Unlike other family members (with one exception), Cvx further oligomerizes to form a multimeric assembly. Cvx is an  $(\alpha\beta)_4$  tetramer and has a structure (Fig. 1) similar to that of flavocetin-A (FL-A), a protein from the venom of *Trimerurus flavoridis* that binds

platelet receptor GPIb (Fukuda *et al.*, 2000). The Cvx  $(\alpha\beta)_4$  tetramer has fourfold crystallographic symmetry and the  $\alpha\beta$ -heterodimers are covalently linked by inter-subunit disulfide bonds between cysteine residues at either end of the long axis of each  $\alpha\beta$ -heterodimer (Fig. 1). These disulfide bonds are formed between Cys133 in the  $\alpha$ -subunit and Cys2 in the

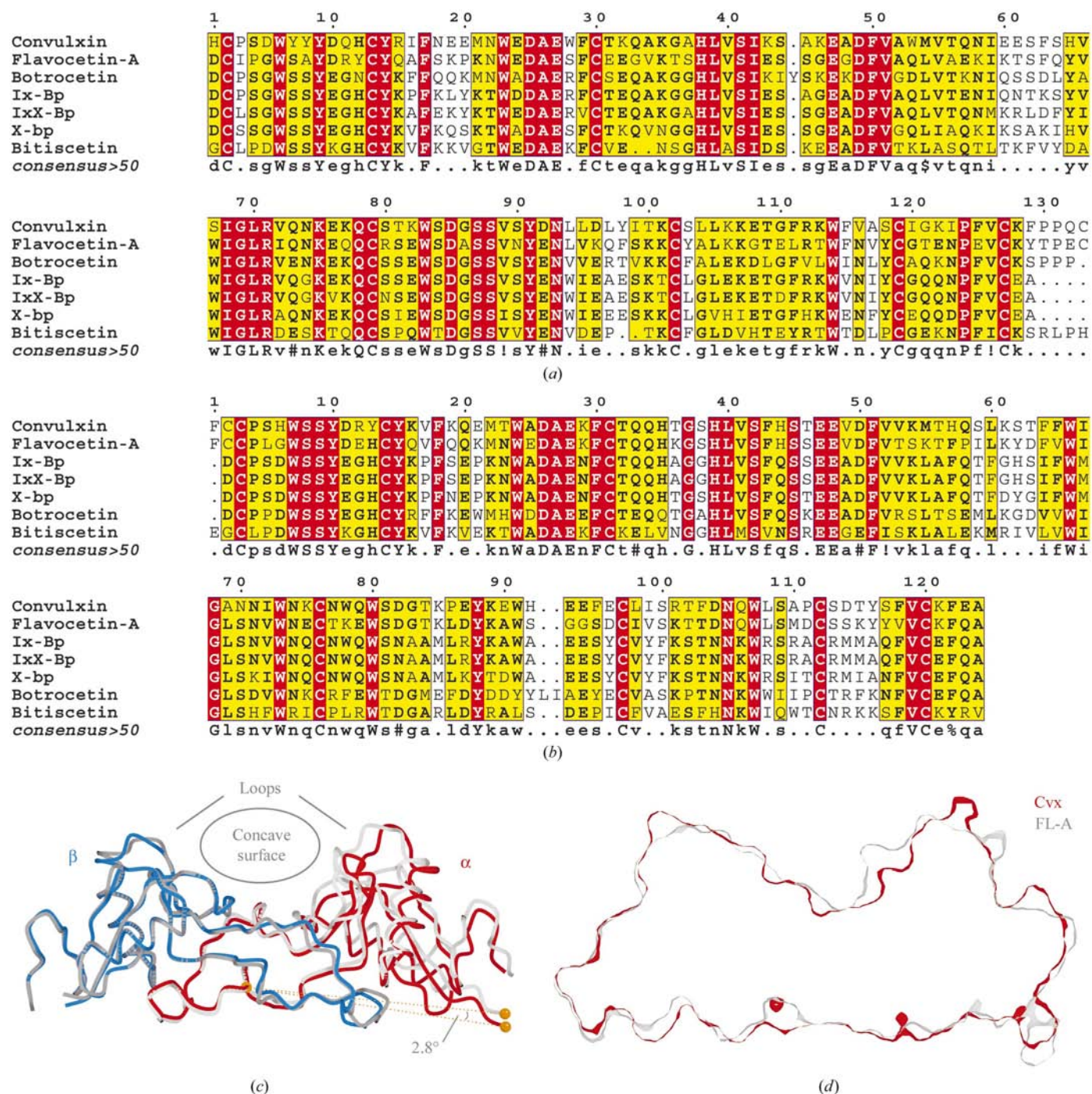


**Figure 2**

Sequence alignment between homologues and comparison of subunit orientations with FL-A. Sequence alignment between several members of the C-type lectin snake-venom family: (a)  $\alpha$ -subunits and (b)  $\beta$ -subunits. (c) Difference in relative orientation of the  $\alpha$ -subunit between FL-A and Cvx, with the  $\beta$ -subunits of both proteins superimposed. The  $\beta$ -subunit and  $\alpha$ -subunit of Cvx are coloured blue and red, respectively. The  $\beta$ -subunit and  $\alpha$ -subunit of FL-A are coloured dark grey and light grey, respectively. The relatively difference in orientation of the  $\alpha$ -subunit is indicated. Non-conserved loop regions and the concave surface implicated in GPVI binding are indicated. (d) Superimposition of the surfaces of Cvx (red) and FL-A (grey) to highlight differences in the concave surface between the two proteins.

$\beta$ -subunit of the neighbouring symmetry-related molecule. The resultant oligomer comprises a  $78 \times 78 \text{ \AA}$  square formation (measuring the distance between  $C^\alpha$  atoms of Cys133 in the  $\alpha$ -subunits; Fig. 1*b*). At present, Cvx and FL-A are the only known C-type lectin snake-venom proteins with an  $(\alpha\beta)_4$  tetrameric structure. The absence of cysteines at the N-terminus of the  $\beta$ -subunit and the C-terminus of the  $\alpha$ -subunit results in single  $\alpha\beta$ -heterodimer molecules in all the other homologous protein structures determined to date (Figs. 2*a* and 2*b*; Mizuno *et al.*, 1997, 1999, 2001; Fukuda *et al.*, 2002; Hirotsu *et al.*, 2001; Sen *et al.*, 2001).

Some C-type lectin snake-venom family members have an  $Mg^{2+}/Ca^{2+}$ -binding site (Mizuno *et al.*, 1999; Hirotsu *et al.*, 2001; Sen *et al.*, 2001). The corresponding residues in Cvx are Ser41, Lys43, Glu47 and Lys128 in the  $\alpha$ -subunit and Ser42, His44, Glu47 and Lys121 in the  $\beta$ -subunit. Although the main-chain topology of the metal-binding site is conserved in Cvx, this function is impaired by the substitution of glutamic acid (required for metal coordination) by lysine at residue 128 in the  $\alpha$ -subunit and residue 121 in the  $\beta$ -subunit. The corresponding site in FL-A is identical (with the exception of Asp at position 43 rather than Lys) and therefore another simi-

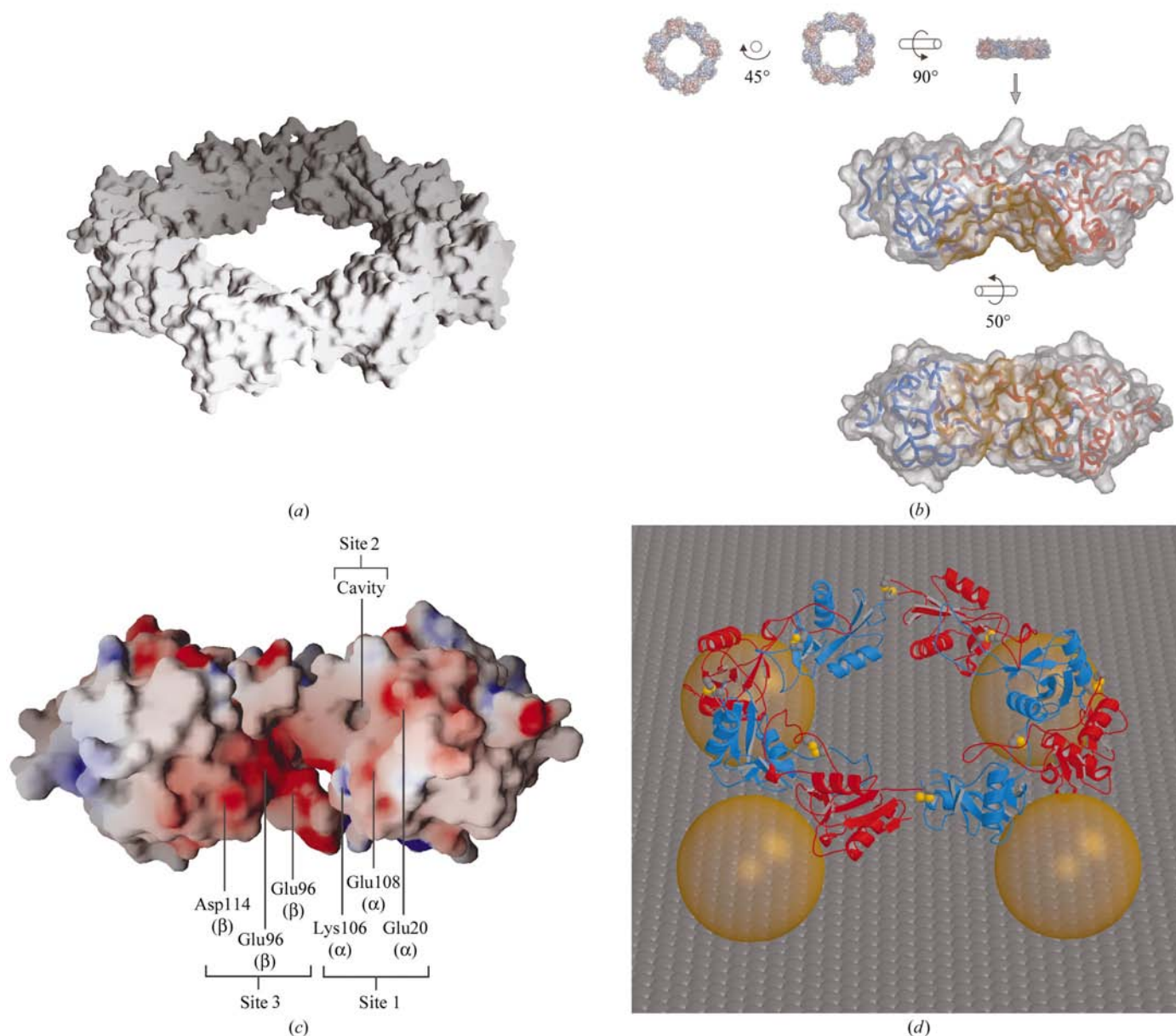


**Figure 3**

Analysis of the concave surface of Cvx. (a) Surface representation of the Cvx tetramer. (b) Orientation of the concave surface relative to the rest of the molecule.  $\beta$ - and  $\alpha$ -subunits are coloured blue and red, respectively. The van der Waals surface of the  $\alpha\beta$ -heterodimer is depicted in transparent grey and the concave surface with a transparent brown tint. Relative orientations of views are given. (c) Close-up view of the concave surface of the  $\alpha\beta$ -heterodimer. Residues contributing to charged patches are indicated. (d) Schematic representation of the Cvx tetramer interaction with protein ligand at the cell surface. The Cvx tetramer is depicted as in Fig. 1(*a*) with a  $120^\circ$  rotation about the horizontal. Ligand molecules interacting at each concave surface are depicted as transparent gold spheres. The cell surface is depicted in grey.

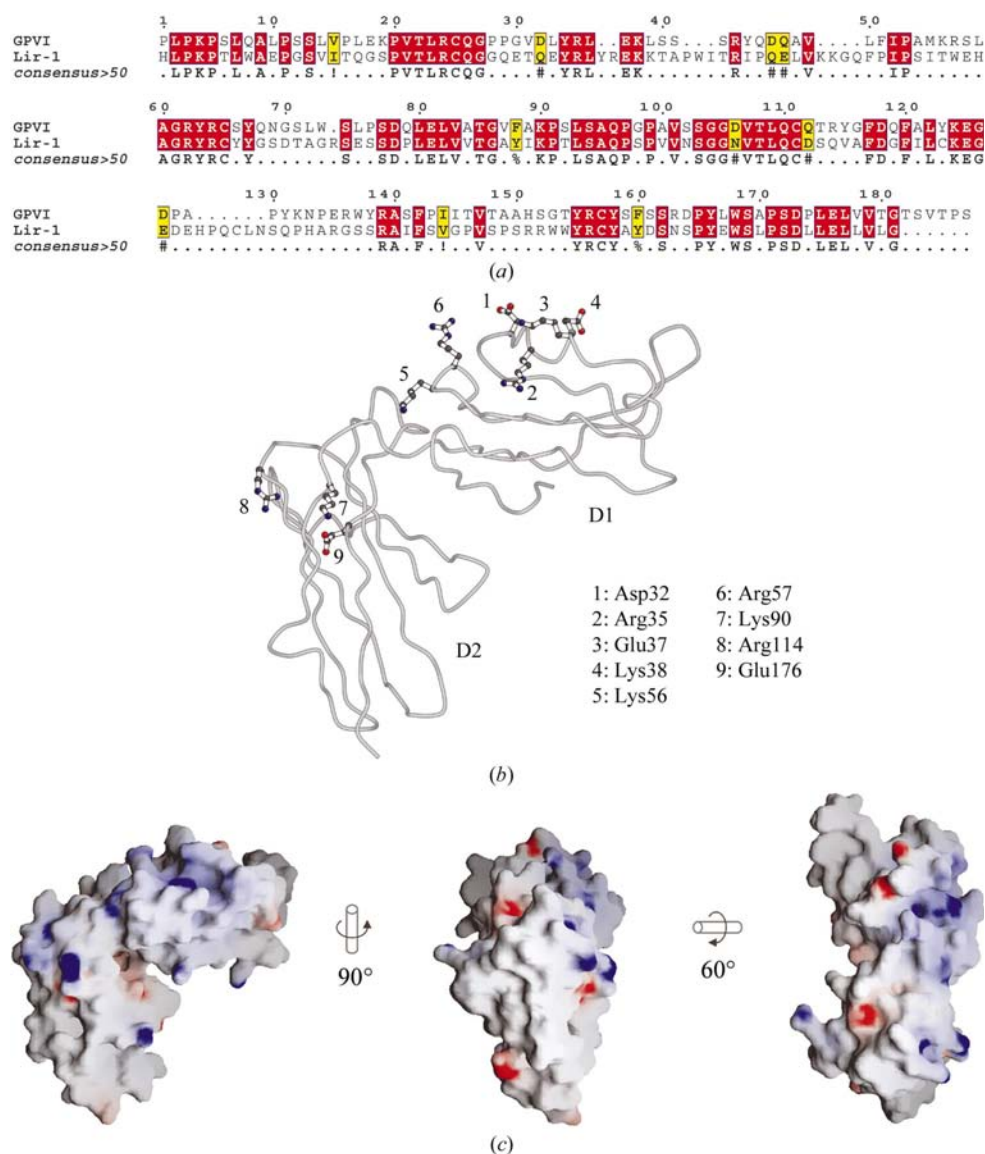


**Figure 4**  
 Homology modelling and analysis of GPVI. (a) Sequence alignment between GPVI and Lir-1. (b) C $\alpha$  trace of the GPVI model in coil representation; side chains of residues contributing to charged patches are drawn in ball-and-stick representation. (c) Surface representation of GPVI model showing distribution of electrostatic potential coloured in blue (positive) and red (negative) viewed in three orientations. The starting orientation is as in (b).

larity between FL-A and Cvx is the absence of Mg<sup>2+</sup>/Ca<sup>2+</sup> binding.

**3.2. The concave surface of the  $\alpha\beta$ -heterodimer**

The  $\alpha\beta$ -heterodimer in C-type lectin snake-venom proteins presents a concave surface which has been predicted to be the binding site for ligands (Hirotsu *et al.*, 2001). This has been confirmed for proteins such as X-bp, botrocetin, bitiscetin and IX-bp by the determination of structures in complex with ligands (Mizuno *et al.*, 2001; Fukuda *et al.*, 2002; Maita *et al.*, 2003; Shikamoto *et al.*, 2003). The relative orientation between the  $\alpha$ - and  $\beta$ -subunits differs by 6–20° in comparisons between family members (Mizuno *et al.*, 1999; Hirotsu *et al.*, 2001; Sen

*et al.*, 2001) and as a result there is a variation in the radius of curvature of the concave surface for different snake-venom proteins. The relative orientation of the  $\alpha$ - and  $\beta$ -subunits in Cvx differs by 2.8° from that in FL-A (Fig. 2c) and therefore the concave surface of Cvx has a somewhat larger radius of curvature than that of FL-A (Fig. 2d). However, this difference in the relative orientation of the  $\alpha$ - and  $\beta$ -subunits is small compared with the differences between family members that do not form oligomeric structures. For example the difference in subunit orientation between bitiscetin and botrocetin is 18° (Hirotsu *et al.*, 2001). For Cvx and FL-A, the range of possible orientations is limited by the additional constraints of tetramer formation.

**3.3. The putative GPVI-binding sites of Cvx**

Within the ( $\alpha\beta$ )<sub>4</sub> tetramer, the concave surfaces of the four  $\alpha\beta$ -heterodimers are angled at ~50° relative to the plane of the ring (Fig. 3a and 3b). This near-diagonal orientation of the putative concave binding sites implies that Cvx would bind a platelet receptor as depicted in Fig. 3(d), docking on top of the cell-surface molecule.

Crystal structures of complexes between the C-type lectin snake-venom proteins and their protein ligands show the site of interaction to be formed by loop regions that fall between the second  $\alpha$ -helix and the second  $\beta$ -strand on both the  $\alpha$ - and  $\beta$ -subunits (Mizuno *et al.*, 2001; Fukuda *et al.*, 2002; Maita *et al.*, 2003; Shikamoto *et al.*, 2003). Sequence alignments between homologues show that these are regions of sequence variability and it is likely that in Cvx, as in other family members, these loops within the concave surface confer specificity in the binding of protein ligand. The analysis of the Cvx structure reveals three potential specificity-conferring sites on the concave surface which may be involved in the interaction with GPVI (Fig. 3c). The first site is on the  $\alpha$ -subunit and consists of two adjacent localized patches of positive and negative charge. The second site is also present on the  $\alpha$ -subunit and is a 5 Å wide cavity lined with residues

Trp23, Ser67, Leu104, Ala117, Gly121 and Ile123. Finally, the third site is a relatively large patch of negative charge on the  $\beta$ -subunit.

Site-directed mutagenesis of the residues Glu20( $\alpha$ ), Lys106( $\alpha$ ), Glu108( $\alpha$ ), Glu94( $\beta$ ), Glu96( $\beta$ ) and Asp114( $\beta$ ) that contribute towards the positive and negative charges of the concave surface will be required to determine their role. It is possible that the hydrophobic cavity on the  $\alpha$ -subunit forms a docking site for a complementary side chain on the protein ligand. This hypothesis can also be tested by site-directed mutagenesis of Ala117 or Gly121 to bulky residues that would presumably fill this cavity.

### 3.4. Key residues on GPVI

Lir-1 and KIR2DL1 are immunoglobulin-superfamily (IgSF) proteins which contain two Ig-like domains, D1 and D2, and have 44 and 35% sequence identity to GPVI, respectively (Figs. 4a and 4b). The crystal structures of both these molecules have been determined and their ligand-binding sites have been identified by site-directed mutagenesis (Chapman *et al.*, 2000; Fan *et al.*, 2001). In both structures the two domains are arranged in tandem, forming a bent structure with an acute interdomain hinge angle. In Lir-1 the residues contributing to the ligand-binding site have been identified in D1 around the N-terminus of the molecule. In KIR2DL1 residues from both D1 and D2 centred around the interdomain hinge have been implicated in ligand binding.

In order to identify potential residues on GPVI that could be involved in the interaction between GPVI and Cvx, a structural model of GPVI was made using the coordinates of Lir-1 as a template and the electrostatic potential of the surface of the model was visualized (Fig. 4). Since most of the putative binding site of Cvx is negatively charged, one would expect a complementary positively charged surface on GPVI. Analysis of the GPVI model shows a region of positive charge spanning D1 and D2, centred around the inter-domain hinge (Fig. 4c). In addition, there are three localized negatively charged patches (residues listed in Fig. 4b), any of which could be the complementary binding site for the positively charged patch on the  $\alpha$ -subunit of Cvx. It is noteworthy that recent experiments using mutant GPVI with collagen-related peptide (CRP) binding assays have mapped the CRP-binding site on GPVI onto the positively charged patch on the hinge surface of D1 (Smethurst *et al.*, 2003). The crystal structure of Cvx now suggests a model for a multimeric signalling assembly formed with GPVI.

*Note added in proof:* A 2.4 Å resolution structure of Cvx has recently been published by Murakami *et al.* (2003) and is in agreement with the features described here.

We thank Bernard Saliou for purification of convulxin. We are grateful to the staff of the SRS (Daresbury), the ESRF and EMBL Outstation (Grenoble) for the assistance with X-ray data collection. We thank Jonathan Grimes, Erika Mancini and Geoff Sutton for help and advice during data collection

and Steve Watson for discussion. This work was funded by the MRC and The European Commission Integrated Programme (SPINE, grant code QLRT-2001-00988). EYJ is a Cancer Research UK Principal Research Fellow.

### References

- Achison, M., Joel, C., Hargreaves, P. G., Sage, S. O., Barnes, M. J. & Farndale, R. W. (1996). *Blood Coagul. Fibrinolysis*, **7**, 149–152.
- Barry, F. A. & Gibbins, J. M. (2002). *J. Biol. Chem.* **277**, 12874–12878.
- Berlanga, O., Tulasne, D., Bori, T., Snell, D. C., Miura, Y., Jung, S., Moroi, M., Frampton, J. & Watson, S. P. (2002). *Eur. J. Biochem.* **269**, 2951–2960.
- Brown, J. *et al.* (2003). *J. Appl. Cryst.* **36**, 315–318.
- Brünger, A. T., Adams, P. D., Clore, G. M., DeLano, W. L., Gros, P., Grosse-Kunstleve, R. W., Jiang, J.-S., Kuszewski, J., Nilges, M., Pannu, N. S., Read, R. J., Rice, L. M., Simonson, T. & Warren, G. L. (1998). *Acta Cryst. D* **54**, 905–921.
- Chapman, T. L., Heikema, A. P., West, A. P. Jr & Bjorkman, P. J. (2000). *Immunity*, **13**, 727–736.
- Cicmil, M., Thomas, J. M., Sage, T., Barry, F. A., Leduc, M., Bon, C. & Gibbins, J. M. (2000). *J. Biol. Chem.* **275**, 27339–27347.
- Clemetson, J. M., Polgar, J., Magnenat, E., Wells, T. N. & Clemetson, K. J. (1999). *J. Biol. Chem.* **274**, 29019–29024.
- Clemetson, K. J. & Clemetson, J. M. (2001). *Thromb. Haemost.* **86**, 189–197.
- Collaborative Computational Project, Number 4 (1994). *Acta Cryst. D* **50**, 760–763.
- Corpet, F. (1988). *Nucleic Acids Res.* **16**, 10881–10890.
- Drickamer, K. (1988). *J. Biol. Chem.* **263**, 9557–9560.
- Esnouf, R. M. (1999). *Acta Cryst. D* **55**, 938–940.
- Fan, Q. R., Long, E. O. & Wiley, D. C. (2001). *Nature Immunol.* **2**, 452–460.
- Francischetti, I. M., Saliou, B., Leduc, M., Carlini, C. R., Hatmi, M., Randon, J., Faili, A. & Bon, C. (1997). *Toxicon*, **35**, 1217–1228.
- Fukuda, K., Doggett, T. A., Bankston, L. A., Cruz, M. A., Diacovo, T. G. & Liddington, R. C. (2002). *Structure*, **10**, 943–950.
- Fukuda, K., Mizuno, H., Atoda, H. & Morita, T. (2000). *Biochemistry*, **39**, 1915–1923.
- Gouet, P., Courcelle, E., Stuart, D. I. & Metoz, F. (1999). *Bioinformatics*, **15**, 305–308.
- Hirotsu, S., Mizuno, H., Fukuda, K., Qi, M. C., Matsui, T., Hamako, J., Morita, T. & Titani, K. (2001). *Biochemistry*, **40**, 13592–13597.
- Humphrey, W., Dalke, A. & Schulten, K. (1996). *J. Mol. Graph.* **14**, 33–38.
- Jones, T. A., Zou, J. Y., Cowan, S. W. & Kjeldgaard, M. (1991). *Acta Cryst. A* **47**, 110–119.
- Kanaji, S., Kanaji, T., Furihata, K., Kato, K., Ware, J. L. & Kunicki, T. J. (2003). *J. Biol. Chem.* **278**, 39452–39460.
- Laskowski, R. A., Moss, D. S. & Thornton, J. M. (1993). *J. Mol. Biol.* **231**, 1049–1067.
- Leduc, M. & Bon, C. (1998). *Biochem. J.* **333**, 389–393.
- Maita, N., Nishio, K., Nishimoto, E., Matsui, T., Shikamoto, Y., Morita, T., Sadler, J. E. & Mizuno, H. (2003). *J. Biol. Chem.* **278**, 37777–37781.
- Marlas, G. (1985). *Biochimie*, **67**, 1231–1239.
- Marlas, G., Joseph, D. & Huet, C. (1983a). *Biochimie*, **65**, 405–416.
- Marlas, G., Joseph, D. & Huet, C. (1983b). *Biochimie*, **65**, 619–628.
- Merritt, E. A. & Bacon, D. J. (1997). *Methods Enzymol.* **277**, 505–524.
- Mizuno, H., Fujimoto, Z., Atoda, H. & Morita, T. (2001). *Proc. Natl Acad. Sci. USA*, **98**, 7230–7234.
- Mizuno, H., Fujimoto, Z., Koizumi, M., Kano, H., Atoda, H. & Morita, T. (1997). *Nature Struct. Biol.* **4**, 438–441.
- Mizuno, H., Fujimoto, Z., Koizumi, M., Kano, H., Atoda, H. & Morita, T. (1999). *J. Mol. Biol.* **289**, 103–112.

- Murakami, M. T., Zela, S. P., Gava, L. M., Michelan-Duarte, S., Cintra, A. C. & Arni, R. K. (2003). *Biochem. Biophys. Res. Commun.* **310**, 478–482.
- Nicholls, A., Sharp, K. A. & Honig, B. (1991). *Proteins*, **11**, 281–296.
- Nieswandt, B. & Watson, S. P. (2003). *Blood*, **102**, 449–461.
- Otwinowski, Z. & Minor, W. (1997). *Methods Enzymol.* **276**, 307–326.
- Polgar, J., Clemetson, J. M., Kehrel, B. E., Wiedemann, M., Magnenat, E. M., Wells, T. N. & Clemetson, K. J. (1997). *J. Biol. Chem.* **272**, 13576–13583.
- Poole, A., Gibbins, J. M., Turner, M., van Vugt, M. J., van de Winkel, J. G., Saito, T., Tybulewicz, V. L. & Watson, S. P. (1997). *EMBO J.* **16**, 2333–2341.
- Sen, U., Vasudevan, S., Subbarao, G., McClintock, R. A., Celikel, R., Ruggeri, Z. M. & Varughese, K. I. (2001). *Biochemistry*, **40**, 345–352.
- Shikamoto, Y., Morita, T., Fujimoto, Z. & Mizuno, H. (2003). *J. Biol. Chem.* **278**, 24090–24094.
- Smethurst, P. A., Joutsu-Korhonen, L., O'Connor, M. N., Jennings, N. S., Wilson, E., Garner, S. F., Knight, C. G., Harmer, I. J., Dafforn, T. R., Ijsseldijk, W. M. J., De Groot, P. G., Watkins, N. A., Farndale, R. W. & Ouwehand, W. H. (2003). *J. Thromb. Haemost.* **1 Suppl.** 1, Abstract No. OC391.
- Stuart, D. I., Levine, M., Muirhead, H. & Stammers, D. K. (1979). *J. Mol. Biol.* **134**, 109–142.
- Vargaftig, B. B., Joseph, D., Wal, F., Marlas, G., Chignard, M. & Chevance, L. G. (1983). *Eur. J. Pharmacol.* **92**, 57–68.
- Vargaftig, B. B., Prado-Franceschi, J., Chignard, M., Lefort, J. & Marlas, G. (1980). *Eur. J. Pharmacol.* **68**, 451–464.
- Walter, T. S., Diprose, J., Brown, J., Pickford, M., Owens, R. J., Stuart, D. I. & Harlos, K. (2003). *J. Appl. Cryst.* **36**, 308–314.